ELSEVIER

www.elsevier.nl/locate/jorganchem

Journal of Organometallic Chemistry 591 (1999) 185–193

Journal of Organometallic Chemistry

# Ancillary aryloxide ligands in ethylene polymerization catalyst precursors

Andrea V. Firth, Jeffrey C. Stewart, Aaron J. Hoskin, Douglas W. Stephan *

*School of Physical Sciences, Chemistry and Biochemistry, University of Windsor, Windsor, ON Canada N9B 3P4*

Received 18 May 1999; accepted 7 July 1999

**Abstract**

The compounds $CpTiCl_2(OC_6H_3\text{-}i\text{-}Pr_2)$ (**1**), $CpTiCl(OC_6H_3\text{-}i\text{-}Pr_2)_2$ (**2**), $CpTi(R)(OC_6H_3\text{-}i\text{-}Pr_2)_2$ (R = *t*-Bu **3**, *s*-Bu **4**, *n*-Bu **5**, Me **6**) have been prepared and characterized. Compounds **1** or **2** in the presence of 500 equivalents of methylaluminoxane (MAO) act as catalyst precursors for ethylene polymerization. While the catalysts derived from the monocyclopentadienyl complexes are much less active that the metallocenes, there is a clear enhancement in the activity of about 40% as a result of the inclusion of a second aryloxide ligand. Reactions of **1** with $AlMe_3$ revealed stepwise formation of $CpTi(Me)Cl(OC_6H_3\text{-}i\text{-}Pr_2)$ **7** and $CpTi(Me)_2(OC_6H_3\text{-}i\text{-}Pr_2)$ **8**, while subsequent addition of $AlMe_3$ afforded complete conversion to **8**, with formation of the aluminum species $[AlMe_2(OC_6H_3\text{-}i\text{-}Pr_2)]_n$ **9**. In contrast, the catecholate complex $CpTi(O_2C_6H_4)Cl$ **10** reacts with $AlMe_3$ yielding the paramagnetic species $[CpTi(O_2(C_6H_4))\cdot AlClMe_2]_2$ **11**. Incorporation of aryloxide ligands in modified metallocenes was readily accomplished with the preparation of $Cp_2ZrCl(OC_6H_3\text{-}i\text{-}Pr_2)$ **12**, $Cp_2ZrCl(OC_6H_5)$ **13**, $Cp_2ZrMe(OC_6H_5)$ **14** and $Cp_2TiCl(OC_6H_3\text{-}i\text{-}Pr_2)$ **15**. In combination with MAO, **12**, **14** and **15** effect the polymerization of ethylene with an 11% increase in activity over the parent metallocenedichlorides. The implications of the increased activity are considered. Crystallographic data are reported for **2**, **3**, **6**, **9**, **11**, **12** and **13**. © 1999 Elsevier Science S.A. All rights reserved.

*Keywords:* Cyclopentadienyl; Titanium; Aryloxide; Ethene polymerization

## 1. Introduction

The utility of metallocenes in olefin polymerization has spawned a variety of approaches to the development of new catalysts. Many have studied metallocene derivatives [1–9] or analogs [10–13], while others have examined half-sandwich complexes such as the so-called 'constrained geometry catalysts (CGC)' of the form $(C_5Me_4SiR_2NR)MX_2$ [14–16]. Still others have adopted the approach based on new catalysts derived from complexes not containing cyclopentadienyl ligands [17–19]. One of our approaches involves the systematic study of a series of less active compounds, with a view to uncovering structural features that can be incorporated into known, highly active systems. In these efforts we began with a focus on the inclusion of ancillary aryloxide ligands. In general, the study of catalysts based on half-sandwich complexes (other than CGC) has received limited attention [20]. We have recently described the chemistry of thiolate derivatives of Cp-Ti(aryloxide) complexes [21–23]; however, it is only in very recent work that Nomura et al. [24] and Repo et al. [25] have examined the utility of some of these species in olefin polymerization catalysis. In this paper, we describe the synthesis, chemistry and olefin polymerization catalysis for several related half-sandwich derivatives containing aryloxide ligands. The lessons learned from the studies of these systems are then applied to metallocene derivatives to effect enhanced catalytic activity.

## 2. Experimental

### 2.1. General data

All preparations were done under an atmosphere of dry, $O_2$-free $N_2$ employing both Schlenk line techniques and an Innovative Technologies or Vacuum Atmo-

* Corresponding author. Fax: +1-519-9737098.
*E-mail address:* stephan@uwindsor.ca (D.W. Stephan)

0022-328X/99/$ - see front matter 
PII: S0022-328X(99)00422-2

spheres inert atmosphere glove box. Solvents were reagent grade, distilled from the appropriate drying agents under $N_2$ and degassed by the freeze–thaw method at least three times prior to use. $^1$H- and $^{13}C\{^1H\}$-NMR spectra were recorded on a Bruker Avance-300 and 500 operating at 300 and 500 MHz for $^1$H spectra, respectively. Trace amounts of protonated solvents were used as references and chemical shifts are reported relative to $SiMe_4$. EPR spectra were recorded employing a Bruker EPS 300e spectrometer equipped with a nuclear magnetometer and a HP frequency counter. Low- and high-resolution EI mass spectral data were obtained employing a Kratos Profile mass spectrometer outfitted with a $N_2$ glove bag enclosure for the inlet port. Galbraith Laboratories, Knoxville, TN or Schwarzkopf Laboratories, Woodside, NY performed combustion analyses. The compound $CpTiCl_3$ was purchased from Strem Chemicals. The compounds $Cp_2ZrMeCl$ [26], $CpTiCl_2Me$ [27], $CpTiCl_2(OC_6H_3$-*i*-$Pr_2)$ **1** [28] and $CpTiCl(O_2C_6H_4)$ **10** [29] were prepared via known methods.

### 2.2. Synthesis of $CpTiCl(OC_6H_3$-*i*-$Pr_2)_2$ (**2**)

To $CpTiCl_3$(2.18 g, 10 mmol) suspended in benzene was added $HOC_6H_3$-*i*-$Pr_2$ (3.56 g, 20 mmol) and imidazole (1.26 g, 20 mmol). The reaction mixture was stirred overnight, then filtered after which the solvent was removed. Orange crystals were obtained in 86% yield from hexane. $^1$H NMR ($C_6D_6$, 25°C) $\delta$: 1.22 (d, 12H, $|J_{H-H}| = 7$ Hz, $CH(CH_3)_2$), 1.26(d, 12H, $|J_{H-H}| = 7$ Hz, $CH(CH_3)_2$), 3.69 (sept, 4H, $|J_{H-H}| = 7$ Hz, $CH(CH_3)_2$), 6.19 (s, 5H, Cp), 6.96(t, 2H, $|J_{H-H}| = 7$ Hz, p-Ar), 7.05 (d, 4H, $|J_{H-H}| = 7$ Hz, m-Ar). $^{13}C\{^1H\}$-NMR ($C_6D_6$, 25°C) $\delta$: 22.9 ($CH(CH_3)_2$), 23.3 ($CH(CH_3)_2$), 25.9($CH(CH_3)_2$), 117.8 (Cp), 122.7(Ar), 122.8(Ar), 137.0(*o*-Ar), 162.9(*ipso*-Ar). HRMS for $C_{29}H_{39}TiO_2Cl$: 502.2118, Found: 502.2120; Anal. Calc.: C: 69.25; H: 7.82; C: 69.15; H: 7.69.

### 2.3. Synthesis of $CpTiR(OC_6H_3$-*i*-$Pr_2)_2$, R = *t*-Bu **3**, *s*-Bu **4**, *n*-Bu **5**, Me **6**

These compounds were prepared in a similar manner and thus only one representative preparation is described. To **2** (95 mg, 0.19 mmol) dissolved in hexane was added *t*-BuLi drop wise (111.7 μl of a 1.7 M solution, 0.19 mmol). The reaction mixture was stirred for a few minutes, then filtered, after which the solvent was reduced. Orange crystals were obtained in 40% yield. **3**: $^1$H-NMR ($C_6D_6$, 25°C)$\delta$: 1.19 (d, 12H, $|J_{H-H}| = 7$ Hz, $CH(CH_3)_2$), 1.22 (d, 12H, $|J_{H-H}| = 7$ Hz, $CH(CH_3)_2$), 1.48(s, 9H, Ti–C($CH_3$)$_3$), 3.67 (sept, 4H, $|J_{H-H}| = 7$ Hz, $CH(CH_3)_2$), 6.18 (s, 5H, Cp), 6.96 (t, 2H, $|J_{H-H}| = 7$Hz, *p*-Ar), 7.07 (d, 4H, $|J_{H-H}| = 7$ Hz, *m*-Ar). $^{13}C\{^1H\}$-NMR ($C_6D_6$, 25°C)$\delta$: 23.6 ($CH(CH_3)_2$), 23.9 ($CH(CH_3)_2$), 25.3 ($CH(CH_3)_2$), 33.5 (Ti–C($CH_3$)$_3$), 82.2 (Ti–$C(CH_3)$), 115.0 (Cp), 121.3 (Ar), 123.0 (Ar), 137.0 (*o*-Ar), 160.5 (*ipso*-Ar). HRMS for $C_{33}H_{48}TiO_2$ 524.3134; Found: 524.3155; Anal. Calc.: C: 75.55; H: 9.22; Found: C:75.29; H: 9.02. **4**: Yield 40%, $^1$H-NMR ($C_6D_6$, 25°C)$\delta$: 1.15–1.2 (m,27H, $CH(CH_3)_2$, $CH(CH_2CH_3)(CH_3)_3$), 1.45 (d, 3H, $|J_{H-H}| = 7$ Hz, $CH(CH_2CH_3)(CH_3)$, 2.10 (d of t, 2H, $|J_{H-H}| = 7$ Hz, $CH(CH_2CH_3)(CH_3)$), 2.61 (t of quart, 1H, $|J_{H-H}| = 7$ Hz, $CH(CH_2CH_3)(CH_3)$, 3.47 (sept, 2H, $|J_{H-H}| = 7$ Hz, $CH(CH_3)_2$), 3.57 (sept, 2H, $|J_{H-H}| = 7$Hz, $CH(CH_3)_2$), 6.17 (s, 5H, Cp), 6.90–6.93 (m, 2H, Ar), 7.02–7.06 (m, 4H, Ar). $^{13}C\{^1H\}$-NMR ($C_6D_6$, 25°C)$\delta$: 22.9 ($CH(CH_2CH_3)(CH_3)$), 24.1 ($CH(CH_3)_2$), 24.2 ($CH(CH_3)_2$), 24.4 ($CH(CH_3)_2$), 24.5 ($CH(CH_3)_2$), 26.7 ($CH(CH_2CH_3)(CH_3)$), 27.1 (($CH(CH_3)_2$) (27.4, $CH(CH_3)_2$, 33.9 ($CH(CH_2CH_3)(CH_3)$), 87.3 ($CH(CH_2CH_3)(CH_3)$), 115.0 (Cp), 119.0 (Ar), 122.2 (Ar), 138.1 (*o*-Ar), 163.3 (*ipso*-Ar). HRMS for $C_{33}H_{48}TiO_2$: 524.3134, Found: 524.3138. **5**: Yield 53%; $^1$H-NMR ($C_6D_6$, 25°C) $\delta$: 1.23–1.25 (m, 29H, $CH(CH_3)_2$ and $CH_2CH_2CH_2CH_3$) 1.98 (m, 4H, $CH_2CH_2CH_2CH_3$), 3.49 (sept, 4H, $|J_{H-H}| = 7$ Hz, $CH(CH_3)_2$), 6.05 (s, 5H, Cp), 6.95 (t, 2H, $|J_{H-H}| = 7$ Hz, *p*-Ar), 7.07(d, 4H, $|J_{H-H}| = 7$ Hz, m-Ar). $^{13}C\{^1H\}$-NMR ($C_6D_6$, 25°C) $\delta$: 12.9 ($CH_2CH_2CH_2CH_3$), 23.2 ($CH(CH_3)_2$), 25.8 ($CH(CH_3)_2$), 27.1 ($CH_2CH_2CH_2CH_3$), 35.3 ($CH_2CH_2CH_2CH_3$), 72.7 ($CH_2CH_2CH_2CH_3$), 113.7 (Cp), 121.2(Ar), 122.8 (Ar), 136.7 (*o*-Ar), 160.4 (*ipso*-Ar). HRMS for $C_{33}H_{48}TiO_2$: 524.3134, Found: 524.3136. **6**: Yield 63%; $^1$H-NMR ($C_6D_6$, 25°C) $\delta$: 1.21 (d, 12H, $|J_{H-H}| = 7$ Hz, $CH(CH_3)_2$), 1.22 (d, 12H, $|J_{H-H}| = 7$ Hz, $CH(CH_3)_2$), 1.39 (s, 3H, Ti–$CH_3$), 3.50 (sept, 4H, $|J_{H-H}| = 7$ Hz, $CH(CH_3)_2$), 6.03 (s, 5H, Cp), 6.95 (t, 2H, $|J_{H-H}| = 7$ Hz, p-Ar), 7.07 (d, 4H, $|J_{H-H}| = 7$ Hz, *m*-Ar). $^{13}C\{^1H\}$-NMR ($C_6D_6$, 25°C) $\delta$: 23.0 ($CH(CH_3)$), 23.8 ($CH(CH_3)$), 26.6 ($CH(CH_3)$), 48.0 (Ti–$CH_3$), 114.6 (Cp), 122.0 (Ar), 123.3 (Ar), 137.4 (*o*-Ar), 161.4 ( *ipso*-Ar). HRMS for $C_{30}H_{42}TiO_2$: 482.2664 Found:482.2663; Anal. Calc.: C: 74.67; H: 8.77; Found: C: 74.55; H: 8.71.

### 2.4. Synthesis of $CpTi(Me)Cl(OC_6H_3$-*i*-$Pr_2)$ (**7**)

(i) To a solution of $CpTiCl_2Me$ (90 mg, 0.45 mmol) in benzene was added $Li(OC_6H_3$-2,6-*i*-$Pr_2)$ (85 mg, 0.45 mmol). The reaction was stirred for 1 h at 25°C and then filtered. The benzene was removed and a yellow solid was crystallised from hexane. (ii) An alternative synthesis of **7** is achieved via the reaction of **1** (200 mg, 0.51 mmol) with $ZnMe_2$ (140 μl of a 2 M solution, 0.28 mmol) in benzene (0.5 ml). The mixture was stirred at 25°C overnight and the solvent removed. The residue was extracted into hexane, filtered and the solvent removed to give the yellow solid in 80% yield. $^1$H-NMR

($C_6D_6$, 25°C)$\delta$: 1.17(d, 6H, $|J_{H-H}| = 7$ Hz, $CH(CH_3)_2$), 1.23 (d, 6H, $|J_{H-H}| = 7$ Hz $CH(CH_3)_2$), 1.48 (s, 3H, $TiCH_3$), 3.28 (sept, 2H, $|J_{H-H}| = 7$ Hz, $CH(CH_3)_2$), 5.93 (s, 5H, Cp), 6.8–6.95 (m, br, 3H, Ar). $^{13}C\{^1H\}$-NMR ($C_6D_6$, 25°C) $\delta$: 23.4 ($CH(CH_3)_2$), 23.5 ($CH(CH_3)_2$), 26.9 ($CH(CH_3)_2$), 61.6 (Ti–$CH_3$) 116.2 (Cp), 123.3 (Ar), 123.4 (Ar), 137.9 (*o*-Ar), 162.1 (*ipso*-Ar). Anal. Calc. for $C_{18}H_{25}ClOTi$: C: 63.45; H: 7.40; Found: C: 63.25; H: 7.19.

### 2.5. Generation of $CpTiMe_2(OC_6H_3$-*i*-$Pr_2)$ (**8**)

To **1** (100 mg, 0.26 mmol) suspended in hexane was added MeMgBr (367 ml of a 1.4 M solution in THF, 0.52 mmol). The reaction mixture was stirred overnight, then filtered, after which the solvent was evaporated. $^1H$-NMR ($C_6D_6$, 25°C) $\delta$: 1.08 (s, 6H, Ti–$(CH_3)_2$), 1.20 (d, 12H, $|J_{H-H}| = 7$ Hz, $CH(CH_3)_2$), 3.33 (sept, 2H, $|J_{H-H}| = 7$ Hz, $CH(CH_3)_2$), 5.90 (s, 5H, *Cp*), 6.98 (t, 1H, $|J_{H-H}| = 7$ Hz, *p*-Ar), 7.10 (d, 2H, $|J_{H-H}| = 7$ Hz, *m*-Ar). $^{13}C\{^1H\}$-NMR ($C_6D_6$, 25°C) $\delta$: 23.5 ($CH(CH_3)_2$), 26.9 ($CH(CH_3)_2$), 54.0 (Ti–$(CH_3)_2$), 113.7 (Cp), 122.2 (Ar), 123.2 (Ar), 137.8 (*o*-Ar), 161.0 (*ipso*-Ar).

### 2.6. Reactions of **1**, **2**, **6**, **7** with $AlMe_3$

These reactions were prepared in a similar manner and thus only one representative preparation is described. **2** (25 mg, 0.05 mmol) dissolved in $C_6D_6$ was added $AlMe_3$ (25 μl (2 M in toluene), 0.05 mmol). The reaction was allowed to stir at 25°C for 12 h and then monitored by NMR spectroscopy.

### 2.7. Synthesis of $[AlMe_2(OC_6H_3$-*i*-$Pr_2)]_2$ (**9**)

To $AlMe_3$ (25 μl, (2 M in toluene), 0.5 mmol) in benzene was added $HOC_6H_3$-*i*-$Pr_2$ (89 mg, 0.5 mmol). Gas evolution was apparent immediately. The solvent was then reduced and white crystals of $(AlMe_2(OR^*))_2$ were observed within 7 days. $^1H$-NMR ($C_6D_8$, 25°C) $\delta$: −0.34 (s, 12H, Al–$CH_3$), 1.26 (d, 24H, $CH(CH_3)_2$), 3.77 (sept, 4H, $|J_{H-H}| = 7$ Hz, $CH(CH_3)_2$), 7.03 (br, 6H, Ar). $^{13}C\{^1H\}$-NMR ($C_6D_8$, 25°C) $\delta$: −0.04 (Al–$CH_3$), 25.7 ($CH(CH_3)_2$), 26.9 ($CH(CH_3)_2$), 125.6 (Ar), 125.8 (Ar), 141.3 (*o*-Ar), 154.1 (*ipso*-Ar). HRMS for $C_{28}H_{46}O_2Al_2$: 468.3128, Found: 468.3143. Anal. Calc.; C: 71.76; H: 9.89; C: 71.66; H: 9.79.

### 2.8. Synthesis of $[CpTi(O_2C_6H_4)\cdot AlClMe_2]_2$ (**11**)

To **10** (100 mg, 0.39 mmol) dissolved in benzene was added $AlMe_3$ (196 μl of a 2 M in toluene, 0.39 mmol). The reaction was allowed to stir at 25°C for 12 h. The solvent was reduced and bright blue crystals of $[CpTi(OC_6H_4O)\cdot AlClMe_2]_2$ were isolated in 73% yield. EPR ($C_6H_6$): $g = 1.979$. HRMS for $C_{26}H_{30}Ti_2O_4Cl_2Al_2$: 594.0212, Found: 594.0239. Calc.: C:49.79; H:4.82; Found: C: 49.59; H: 4.73.

### 2.9. Synthesis of $Cp_2ZrCl(OC_6H_3$-*i*-$Pr_2)$ (**12**) and $Cp_2ZrCl(OC_6H_5)$ (**13**)

These compounds were prepared in a similar fashion and thus one representative preparation is presented. To $Cp_2ZrHCl$ (100 mg 0.39 mmol) in benzene was added $HOC_6H_3$-*i*-$Pr_2$ (89 mg, 0.5 mmol). Gas evolution was apparent immediately. After 2 h, the solvent volume was reduced and white crystals of **12** were obtained. **12**: $^1H$-NMR ($C_6D_8$, 25°C) $\delta$: 1.26 (d, 12H, $|J_{H-H}| = 7$ Hz, $CH(CH_3)_2$), 3.30 (sept, 2H, $|J_{H-H}| = 7$ Hz, $CH(CH_3)_2$), 5.97 (s, 10, Cp), 7.03 (m, 3H, Ar). $^{13}C\{^1H\}$-NMR ($C_6D_8$, 25°C) $\delta$: 24.3 ($CH(CH_3)_2$), 30.4 ($CH(CH_3)_2$), 113.5 (Cp), 121.0 (Ar), 123.9 (Ar), 136.3 (*o*-Ar), 160.0 (*ipso*-Ar). Calc. for $C_{22}H_{27}ClOZr$; C: 60.87; H:6.27; Found: C: 60.64; H: 6.17. **13**: $^1H$-NMR ($C_6D_6$, 25°C, $\delta$): 7.19 (t, 2H, $|J_{H-H}| = 7$ Hz, Ar), 6.85 (t, 1H, $|J_{H-H}| = 7$ Hz, Ar), 6.68 (d, 2H, $|J_{H-H}| = 7$ Hz, Ar), 5.93 (s, 10H, Cp).

### 2.10. Synthesis of $Cp_2ZrMe(OC_6H_5)$ (**14**)

To an off-white mixture of 85 mg (0.335 mmol) $Cp_2ZrMeCl$ in benzene was added a bright white suspension of 34 mg (0.340 mmol) $LiOC_6H_5$ in benzene. The mixture was stirred for 15 h and filtered. The straw-yellow filtrate was evaporated to give an off-white oily solid in 74% yield. $^1H$-NMR ($C_6D_6$, 25°C, $\delta$): 7.19 (t, 2H, $|J_{H-H}| = 7$ Hz, Ar), 6.84 (t, 1H, $|J_{H-H}| = 7$ Hz, Ar), 6.58 (d, 2H, $|J_{H-H}| = 7$ Hz, Ar), 5.75 (s, 10H, *Cp*), 0.46 (s, 3H, Me). $^{13}C\{^1H\}$-NMR ($C_6D_6$, 25°C, $\delta$): 165.4 (*ipso*-Ar), 129.6 (Ar), 119.5 (Ar), 118.2 (Ar), 111.2 (Cp), 22.4 (Me).

### 2.11. Synthesis of $Cp_2TiCl(OC_6H_3$-*i*-$Pr_2)$ (**15**)

To $Cp_2TiCl_2$ (100 mg 0.18 mmol) in benzene was added $HOC_6H_3$-*i*-$Pr_2$ (32.1 mg, 0.18 mmol) and $NEt_3$ (35 μl, 0.25 mmol). The mixture was allowed to stir for 12 h, then filtered. After the solvent was removed, an orange solid was obtained in 62% yield. $^1H$-NMR ($C_6D_8$, 0°C) $\delta$: 1.23 (d, 6H, $|J_{H-H}| = 7$ Hz, $CH(CH_3)_2$), 1.61 (d, 6H, $|J_{H-H}| = 7$ Hz, $CH(CH_3)_2$), 2.90 (sept, 2H, $|J_{H-H}| = 7$ Hz, $CH(CH_3)_2$), 4.82 (sept, 2H, $|J_{H-H}| = 7$ Hz, $CH(CH_3)_2$) 6.00 (s, 10H, Cp), 7.04–7.12 (3t, 3H, Ar). $^{13}C\{^1H\}$-NMR ($C_6D_8$, 25°C) $\delta$: 23.0 ($CH(CH_3)_2$), 25.3 ($CH(CH_3)_2$), 110.3 (Cp), 118.9 (Ar), 122.4 (Ar), 134.6 (*o*-Ar), 164.1 (*ipso*-Ar). Calc. for $C_{22}H_{27}ClOTi$; C: 67.61; H:6.96; Found: C: 67.49; H: 6.89.

### 2.12. X-ray data collection and reduction

X-ray-quality crystals of **2**, **3**, **6**, **9**, **11**–**13** were obtained directly from the preparations described above. The crystals were manipulated and mounted in capillaries in a glove box, thus maintaining a dry, $O_2$-free environment for each crystal. Diffraction experiments were performed on a Rigaku AFC6 diffractometer equipped with graphite-monochromatized Mo–$K_\alpha$ radiation. The initial orientation matrices were obtained from 20 machine-centered reflections selected by an automated peak search routine. These data were used to determine the crystal systems. Automated Laue system check routines around each axis were consistent with the crystal system. Ultimately, 25 reflections ($20 < 2\theta < 25°$) were used to obtain the final lattice parameters and the orientation matrices. Crystal data are summarized in Table 1. The observed extinctions were consistent with the space groups in each case. The data sets were collected in three shells ($4.5 < 2\theta < 45–50.0°$) and three standard reflections were recorded every 197 reflections. Fixed scan rates were employed. Up to four repetitive scans of each reflection at the respective scan rates were averaged to insure meaningful statistics. The number of scans of each reflection was determined by the intensity. The intensities of the standards showed no statistically significant change over the duration of the data collections. The data were processed using the TEXSAN crystal solution package operating on an SGI Challenge mainframe computer with remote X-terminals. The reflections with $F_o^2 > 3\sigma F_o^2$ were used in the refinements.

### 2.13. Structure solution and refinement

Non-hydrogen atomic scattering factors were taken from the literature tabulations [30,31]. The heavy atom positions were determined using direct methods employing either the SHELX-86 or Mithril direct methods routines. The remaining non-hydrogen atoms were located from successive difference Fourier map calculations. The refinements were carried out by using full-matrix least squares techniques on $F$, minimizing the function $\omega(|F_o| - |F_c|)^2$ where the weight $\omega$ is defined as $4F_o^2/2\sigma(F_o^2)$ and $F_o$ and $F_c$ are the observed and calculated structure factor amplitudes. In the final cycles of each refinement, the number of non-hydrogen atoms assigned anisotropic temperature factors was determined so as to maintain a reasonable data:variable ratio. The remaining atoms were assigned isotropic temperature factors. In some instances the geometries of the cyclopentadienyl and phenyl rings were also constrained to maintain a statistically meaningful data:variable ratio. Where appropriate, empirical absorption corrections were applied to the data sets based on psi-scan data and employing the software resident in the TEXSAN package. Hydrogen atom positions were calculated and allowed to ride on the carbon to which they are bonded assuming a C–H bond length of 0.95 Å. Hydrogen atom temperature factors were fixed at

Table 1
Crystallographic parameters [a]

| | **2** | **3** | **6** | **9** | **11** | **12** | **13** |
|---|---|---|---|---|---|---|---|
| Formula | $C_{29}H_{39}O_2TiCl$ | $C_{33}H_{48}O_2Ti$ | $C_{30}H_{42}O_2Ti$ | $C_{28}H_{46}O_2Al_2$ | $C_{26}H_{30}O_4Al_2Cl_2Ti_2$ | $C_{22}H_{27}ClOZr$ | $C_{16}H_{15}ClOZr$ |
| Formula weight | 502.98 | 524.64 | 482.56 | 468.63 | 621.04 | 434.0 | 350.0 |
| $a$ (Å) | 10.364(3) | 17.725(9) | 12.264(2) | 17.536(7) | 16.540(4) | 10.621(3) | 14.514(5) |
| $b$ (Å) | 16.245(3) | 11.039(4) | 22.128(4) | 9.606(3) | 21.237(2) | 17.994(7) | 14.217(4) |
| $c$ (Å) | 9.786(3) | 19.761(8) | 10.471(2) | 18.061(3) | 8.470(2) | 11.186(3) | 15.201(9) |
| $\alpha$ (°) | 100.49(2) | | | | | | |
| $\beta$ (°) | 117.93(2) | 125.35(3) | | 93.23(2) | | 90.38(2) | 105.36(3) |
| $\gamma$ (°) | 84.36(2) | | | | | | |
| $V$ (Å$^3$) | 1431.2(7) | 3153(2) | 2841.8(9) | 3037(1) | 2975(1) | 2137(1) | 3024(2) |
| Space group | $P$-1 | $Cc$ | $Pnma$ | $P2_1/a$ | $Pbca$ | $P2_1/n$ | $P2_1/a$ |
| $D_{calc.}$ (g cm$^{-1}$) | 1.167 | 1.105 | 1.128 | 1.025 | 1.387 | 1.349 | 1.537 |
| $Z$ | 2 | 4 | 4 | 4 | 8 | 4 | 8 |
| $\mu$ (mm$^{-1}$) | 0.414 | 0.296 | 0.318 | 0.115 | 0.804 | 0.637 | 0.892 |
| Scan speed (° min$^{-1}$) | 8.0 | 16.0 | 32.0 | 16.0 | 32.0 | 32.0 | 16 |
| Data collected | 5364 | 3055 | 2872 | 1476 | 3000 | 4141 | 5808 |
| $2\theta$/index ranges | 4.5–50 | 4.5–50 | 4.5–50 | 4.5–50 | 4.5–45 | 4.5–50 | 4.5–50.0 |
| Data $F_o^2 > 3\sigma(F_o^2)$ | 1627 | 704 | 732 | 1446 | 1099 | 1271 | 825 |
| Variables | 213 | 115 | 81 | 169 | 163 | 116 | 97 |
| $R$ (%) [b] | 4.50 | 5.90 | 9.80 | 5.40 | 3.33 | 5.90 | 7.50 |
| $wR$ (%) [b] | 6.80 | 9.60 | 9.77 | 8.40 | 4.90 | 7.90 | 8.50 |
| Goodness-of-fit | 1.77 | 2.63 | 2.76 | 2.28 | 1.50 | 2.16 | 1.90 |

[a] All data collected at 24°C with Mo–$K_\alpha$ radiation ($\lambda = 0.71069$ Å), a scan range of 1.0 above $K_{\alpha_1}$ and 1.0 below $K_{\alpha_1}$, with a background to scan ratio of 0.5.

[b] $R = \Sigma||F_o| - |F_c||/\Sigma|F_o|$, $wR = [\Sigma(|F_o| - |F_c|)^2|/\Sigma|F_o|^2]^{0.5}$.

1.10 times the isotropic temperature factor of the carbon atom to which they are bonded. The hydrogen atom contributions were calculated, but not refined. Inversion and refinement of the model confirmed where appropriate the correct enantiomorph of the models. The final values of $R$, $wR$ and the goodness of fit in the final cycles of the refinements are given in Table 1. The locations of the largest peaks in the final difference Fourier map calculation as well as the magnitude of the residual electron densities in each case were of no chemical significance. CIF tables have been deposited as supplementary material.

### 2.14. Ethylene polymerization

A solution of 6–10 μmol of catalyst in 2.0 ml of dry toluene was added to a flask containing 2.0 ml of dry toluene. 500 equivalents of a 10% by weight toluene solution of methylaluminoxane (MAO) was added to the flask. The flask was attached to a Schlenk line with cold trap, a stopwatch was started and the flask was three times evacuated for five seconds and refilled with pre-dried 99.9% ethylene gas. The solution was rapidly stirred under 1 atmosphere of ethylene at room temperature. The polymerization was stopped by the injection of a 1.0 M HCl + methanol solution and total reaction time was noted. The polymer was filtered and washed with copious amounts of water and placed on a drying oven for subsequent weighing.

## 3. Results and discussion

The compounds $CpTiCl_2(OC_6H_3\text{-}i\text{-}Pr_2)_2$ (**1**) was prepared by known methods [24] while $CpTiCl(OC_6H_3\text{-}i\text{-}Pr_2)_2$ (**2**) was obtained by a modification of the known route. Spectroscopic characterizations of both **1** and **2** were as expected. Crystallographic data confirmed the formulations and revealed little variation in the Ti–O bond distances or in the Ti–O–C angles (Fig. 1). The two Ti–O distances for **2** are similar (1.793(5) and 1.809(6) Å) and yet the Ti–O–C angles differ substantially at 170.3(6) and 149.3(6)°. Although it is tempting to suggest this difference may result from differing degrees of π-donation from the phenoxide ligands to the metal center, one cannot dismiss simple steric crowding as the cause.

Alkylation of **2** is achieved via treatment with a variety of alkyl lithium reagents (Scheme 1). This is in contrast to the reaction of **1** with BuLi which results in reduction to what is presumed to be a Ti(III) species. Treating **2** with $t$-BuLi yielded the orange crystalline solid **3** in 40% yield. $^1$H- and $^{13}$C{$^1$H}-NMR spectral data included resonances at 1.48 and 82.8 ppm. respectively. X-ray crystallographic analysis of **3** confirmed the formulation as $CpTi(t\text{-}Bu)(OC_6H_3\text{-}i\text{-}Pr_2)_2$ (Fig. 2).

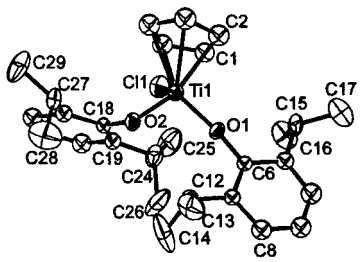


Fig. 1. ORTEP drawing of **2**; 30% thermal ellipsoids are shown and hydrogen atoms are omitted for clarity. Ti(1)–Cl(1) 2.292(3) Å; Ti(1)–O(1) 1.793(5) Å; Ti(1)–O(2) 1.809(6) Å; O(1)–C(6) 1.365(9) Å; O(2)–C(18) 1.357(9) Å; Cl(1)–Ti(1)–O(1) 102.2(2)°; Cl(1)–Ti(1)–O(2) 103.2(2)°; O(1)–Ti(1)–O(2) 103.0(3)°; Ti(1)–O(1)–C(6) 170.3(6)°; Ti(1)–O(2)–C(18) 149.3(6)°.

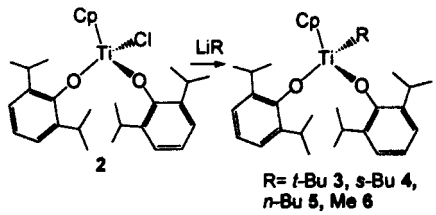


Scheme 1.

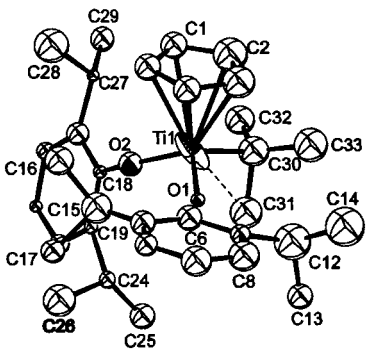


Fig. 2. ORTEP drawing of **3**; 30% thermal ellipsoids are shown and hydrogen atoms are omitted for clarity. Ti(1)–O(1) 1.79(2) Å; Ti(1)–O(2) 1.79(2) Å; Ti(1)–C(30) 1.97(4) Å; Ti(1)–C(31) 2.66(4) Å; O(1)–C(6) 1.42(2) Å; O(2)–C(18) 1.34(2) Å; O(1)–Ti(1)–O(2) 107.7(9)°; O(1)–Ti(1)–C(30) 115(1)°; O(1)–Ti(1)–C(31) 94(1)°; O(2)–Ti(1)–C(30) 108(1)°; O(2)–Ti(1)–C(31) 89(1)°; Ti(1)–O(1)–C(6) 153(1)°; Ti(1)–O(2)–C(18) 156(1)°; Ti(1)–C(30)–C(31) 96(2)°; Ti(1)–C(31)–C(30) 47(1)°.

The Ti–O distance and Ti–O–C angle are similar to those in **1** and **2**. The Ti(1)–C(30) and Ti(1)–C(31) distances of 1.97(4) and 2.66(4) Å suggest an agostic interaction of the Lewis acidic metal center with a C–H bond. Nonetheless, the crystallographic data did not confirm this as the methyl hydrogen atoms could not be located. Moreover, no evidence of such an agostic interaction was evident in the NMR spectral data even at −80°C.

In analogous reactions of **2** with $s$-BuLi, $n$-BuLi and MeLi, the species $CpTi(s\text{-}Bu)(OC_6H_3\text{-}i\text{-}Pr_2)_2$ **4** $CpTi(n\text{-}Bu)(OC_6H_3\text{-}i\text{-}Pr_2)_2$ **5** and $CpTi(Me)(OC_6H_3\text{-}i\text{-}Pr_2)_2$ **6** respectively were obtained. X-ray crystallographic

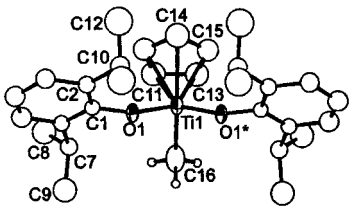


Fig. 3. ORTEP drawing of **6**; 30% thermal ellipsoids are shown and hydrogen atoms are omitted for clarity. Ti(1)–O(1) 1.817(9) Å; Ti(1)–C(16) 2.08(3) Å; O(1)–C(1) 1.40(2) Å; O(1)–Ti(1)–O(1)′ 109.0(5)°; O(1)–Ti(1)–C(16) 100.5(5)°.

analysis of **6** confirmed the formulation (Fig. 3). Interestingly, in this case the two Ti-phenoxide fragments are identical as this molecule sits on a crystallographic mirror. The Ti–C distance (2.00(3) Å) is within the experimental error of that seen in **3**.

Compounds **1** or **2** in the presence of 500 equivalents of MAO act as catalyst precursors for ethylene polymerization (Table 2). In our experiments, 5–10 μmol of catalyst precusor were dissolved in 4.0 ml of toluene and 500 equivalents of MAO were added under an $N_2$ atmosphere. Ethylene was introduced via three successive pump (5 s)–fill cycles. Following the final fill cycle the solution was allowed to stir under the ethylene atmosphere. After 3 min, the catalysis was quenched via addition of a solution of 1 M aqueous HCl + methanol. The reaction times were limited to preclude catalyst entrapment in the polyethylene. The resulting polyethylene was isolated via filtration, washed with water, dried to constant weight, and subsequently characterized by GPC. In order to ensure experimental consistency, catalyst activities were measured in duplicate and standardized against the activity of $Cp_2ZrCl_2$ (1 min). These data revealed that the catalysts derived from the monocyclopentadienyl complexes are much less active than the metallocenes. As well, these activities are significantly lower than Nomura et al. [24] observed under higher pressures of ethylene. Nonetheless, the present results show a clear enhancement in the activity of about 40% as a result of the inclusion of a

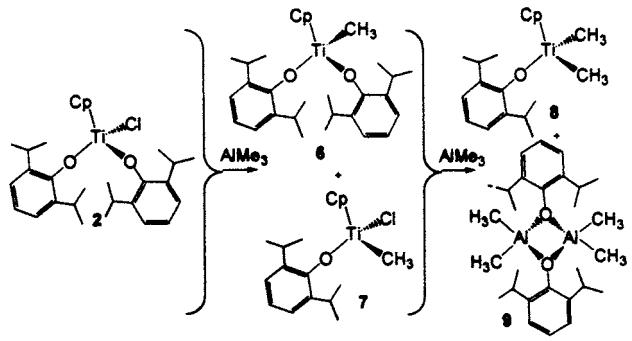


Scheme 2.

second aryloxide ligand in the catalyst precursor **2**. The GPC data also indicate significant differences in molecular weight of the resulting polymers. For example, while $Cp_2ZrCl_2$ affords polymer of molecular weight ($M_w$) of approximately 100 000, a polymer of $M_w$ 300 000 is obtained from **1**. Despite this difference, the polydispersities of the polymers obtained are essentially unchanged.

In an effort to model the catalytic system, stoichiometric reactions with $AlMe_3$ were examined. Monitoring of the reactions of **1** with 1, 2 and excess equivalents of $AlMe_3$ revealed the stepwise formation of Cp-Ti(Me)Cl($OC_6H_3$-*i*-$Pr_2$) (**7**) and $CpTi(Me)_2$($OC_6H_3$-*i*-$Pr_2$) (**8**) with the by-product $AlMe_2Cl$ (Scheme 2). This was confirmed by the synthesis of authentic samples of **7** and **8**. The analogous reactions of **2** also lead initially to a mixture of **6**, **7** and **8** as confirmed by NMR data. It appears that the initial reaction of **2** has two viable pathways, methyl-halide exchange and aryloxide abstraction. Addition of a second equivalent of $AlMe_3$ afforded conversion of **6** and **7** to **8**.

The course of aryloxide group transfer was confirmed via an independent synthesis of the aluminum species $[AlMe_2(OC_6H_3$-*i*-$Pr_2)]_n$ **9**. This was achieved via treatment of $AlMe_3$ with one equivalent of $HOC_6H_3$-*i*-$Pr_2$. The colorless solid **9** was isolated following the evaporation of the solvent. $^1$H- and $^{13}C\{^1H\}$-NMR spectra of **9** were consistent with the empirical formulation and

Table 2
Polymerization results

| Catalyst | Related activity [a] | Time (min) | $M_w$ (Daltons) | $M_w/M_n$ |
|---|---|---|---|---|
| $CpTiCl_2(OC_6H_3$-*i*-$Pr_2)$ (**1**) | 0.11 | 3 | 336 866 | 2.65 |
| $CpTiCl(OC_6H_3$-*i*-$Pr_2)_2$ (**2**) | 0.16 | 3 | 110 000 | 2.20 |
| $CpTi(Me)(OC_6H_3$-*i*-$Pr_2)_2$ (**6**) | 0.16 | 3 | 160 300 | 2.18 |
| $Cp_2ZrCl_2$ | 1.00 | 1 | 116 353 | 2.84 |
| $Cp_2ZrCl(OC_6H_3$-*i*-$Pr_2)$ (**12**) | 1.11 | 1 | 23 200 | 2.48 |
| $Cp_2ZrMe(OC_6H_5)$ (**14**) | 1.11 | 1 | – | – |
| $Cp_2TiCl_2$ | 0.77 | 1 | 69 500 | 6.88 |
| $Cp_2TiCl(OC_6H_3$-*i*-$Pr_2)$ (**15**) | 0.85 | 1 | 40 700 | 3.99 |

[a] Catalyst activities are reported relative to that observed for $Cp_2ZrCl_2$ in the presence of 500 equivalents of MAO at 25°C and 1 atm of ethylene. Under these conditions the activity of $Cp_2ZrCl_2$/MAO was 795 g of PE/mmol of catalyst/h.

crystallographic analysis confirmed the dimeric nature (Fig. 4), in which two aluminum centers are bridged by two phenoxide oxygen atoms. The Al–O and Al–C distances were similar to those seen in the analogous species $[AlMe_2(\mu\text{-}OC_6H_2\text{-}2,4,6\text{-}t\text{-}Bu_3)]_2$ [32]. Compound **9** is the sole aluminum product in the reactions of **2** with $AlMe_3$.

The related catecholate complex $CpTi(O_2C_6H_4)Cl$ **10** was prepared as described in the literature [26]. This species is a structural relative of **2** although the chelating nature of the catechol ligand was expected to alter the reaction pathway with $AlMe_3$. Treatment of **9** with one equivalent of $AlMe_3$ resulted in a dark solution over a period of several days. Blue crystals of the

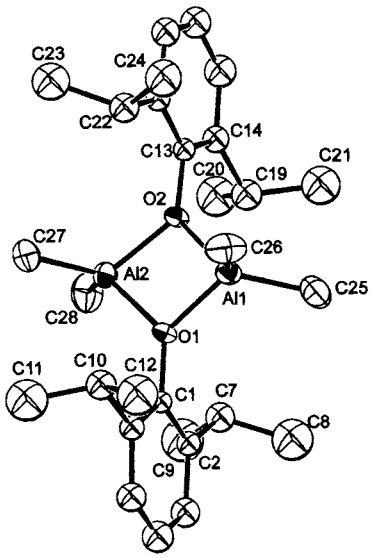


Fig. 4. ORTEP drawing of **9**; 30% thermal ellipsoids are shown and hydrogen atoms are omitted for clarity. Al(1)–O(1) 1.862(7) Å; Al(1)–O(2) 1.852(7) Å; Al(1)–C(25) 1.93(1) Å; Al(1)–C(26) 1.95(1) Å; Al(2)–O(1) 1.861(7) Å; Al(2)–O(2) 1.877(7) Å; Al(2)–C(27) 1.93(1) Å; Al(2)–C(28) 1.95(1) Å; O(1)–C(1) 1.40(1) Å; O(2)–C(13) 1.43(1) Å; O(1)–Al(1)–O(2) 80.2(3)°; O(1)–Al(1)–C(25) 115.4(5)°; O(1)–Al(1)–C(26) 113.8(5)°; O(2)–Al(1)–C(25) 117.5(5)°; O(2)–Al(1)–C(26) 111.4(4)°; C(25)–Al(1)–C(26) 114.3(6)°; O(1)–Al(2)–O(2) 79.6(3)°; O(1)–Al(2)–C(27) 113.0(4)°; O(1)–Al(2)–C(28) 115.8(4)°; O(2)–Al(2)–C(27) 113.7(4)°; O(2)–Al(2)–C(28) 115.1(5)°; C(27)–Al(2)–C(28) 114.9(5)°; Al(1)–O(1)–Al(2) 99.8(4)°; Al(1)–O(1)–C(1) 130.0(6)°; Al(2)–O(1)–C(1) 130.2(6)°; Al(1)–O(2)–Al(2) 99.6(4)°; Al(1)–O(2)–C(13) 132.7(6)°; Al(2)–O(2)–C(13) 127.7(6)°.

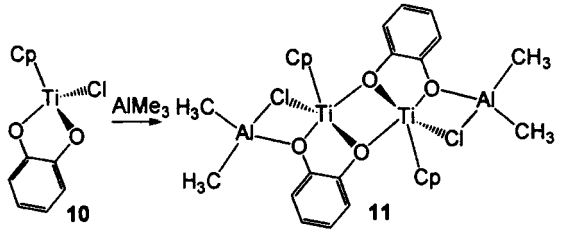


Scheme 3.

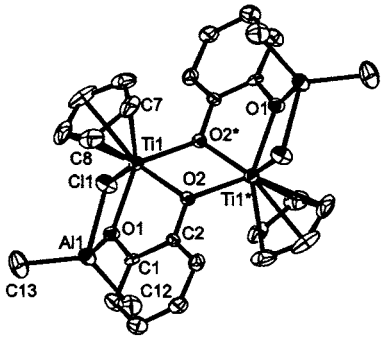


Fig. 5. ORTEP drawing of **11**; 30% thermal ellipsoids are shown and hydrogen atoms are omitted for clarity. Ti(1)–Cl(1) 2.541(3) Å; Ti(1)–O(1) 2.079(5) Å; Ti(1)–O(2) 2.059(4) Å; Ti(1)–O(2) 2.063(5) Å; Cl(1)–Al(1) 2.275(3) Å; Al(1)–O(1) 1.842(5) Å; Al(1)–C(12) 1.948(9) Å; Al(1)–C(13) 1.934(8) Å; O(1)–C(1) 1.387(7) Å; O(2)–C(2) 1.371(7) Å; Cl(1)–Ti(1)–O(1) 75.2(2)°; Cl(1)–Ti(1)–O(2) 128.1(1)°; Cl(1)–Ti(1)–O(2) 89.4(2)°; O(1)–Ti(1)–O(2) 76.1(2)°; O(1)–Ti(1)–O(2) 127.4(2)°; O(2)–Ti(1)–O(2) 75.2(2)°; Ti(1)–Cl(1)–Al(1) 85.3(1)°; Cl(1)–Al(1)–O(1) 86.7(2)°; Cl(1)–Al(1)–C(12) 109.5(3)°; Cl(1)–Al(1)–C(13) 110.3(3)°; O(1)–Al(1)–C(12) 110.0(3)°; O(1)–Al(1)–C(13) 111.2(4)°; C(12)–Al(1)–C(13) 123.2(4)°; Ti(1)–O(1)–Al(1) 112.8(3)°; Ti(1)–O(1)–C(1) 113.2(4)°; Al(1)–O(1)–C(1) 128.2(5)°; Ti(1)–O(2)–Ti(1) 104.8(2)°; Ti(1)–O(2)–C(2) 115.2(4)°; Ti(1)–O(2)–C(2) 133.7(4)°.

paramagnetic complex **11** ($g = 1.197$) were isolated in 73% yield. This species was subsequently characterized as $[CpTi(O_2(C_6H_4))\cdot AlClMe_2]_2$ **11** by crystallographic methods (Scheme 3, Fig. 5). Complex **11** is a bimetallic bridged species in which one of the oxygen atoms of each catecholate ligands bridge the two Ti(III) centers forming a $Ti_2O_2$ core. The average Ti–O distances within this core is 2.069(5) Å. The second oxygen atom of the catecholates, as well as a chloride atom, bridge the titanium and aluminum centers. These Ti–O distances of 2.063(5) Å are indistinguishable from those in the core. The Ti–Cl distance of 2.541(2) Å is quite long compared to those of $CpTiCl_3$ (2.25 Å), consistent with an $AlCl_2Me$ adduct of the Ti(III) centers. The relative disposition of the cyclopentadienyl ligands in the $Ti_2Al_2$ species is *transoid*. The mechanism by which **10** is reduced is unknown. Speculation suggests a process in which association of **10** with $AlMe_3$ is followed by a bimetallic reductive elimination of ethane.

The above observations create a picture in which initial association of aluminum reagents with aryloxide ligands promotes ligand abstraction. This, of course, is subverted by the chelate effect in the case of **10**. For the aryloxide complexes this process occurs for both stoichiometric and catalytic reaction conditions. The increase in catalytic activity of **2** over **1** prompts the question as to whether such ligand incorporation will have the same effect in catalysts where the activity is in a higher regime. This prompted us to prepare modified metallocenes. An alternative synthesis of the known species $Cp_2ZrCl(OC_6H_3\text{-}i\text{-}Pr_2)$ **12** [25] was derived from

treating $Cp_2ZrHCl$ with $HOC_6H_3$-*i*-$Pr_2$ (Scheme 4). Subsequent solvent removal afforded colorless crystals of **12**. NMR data were consistent with the formulation of **12** as $Cp_2ZrCl(OC_6H_3$-*i*-$Pr_2)$. X-ray crystallography confirmed this formulation (Fig. 6). The Zr–O of 1.97(1) Å and the Zr–O–C angle of 172(1)° are typical, suggesting some π-interaction between Zr and O. The analogous compounds $Cp_2ZrCl(OC_6H_5)$ **13** was prepared in an similar manner. X-ray data for **13** (Fig. 7) revealed that the Zr–O distance in **13** (1.99(3) Å) was similar to that seen in **12** despite the fact that the ZrO–C angle is diminished to 150(2)°.

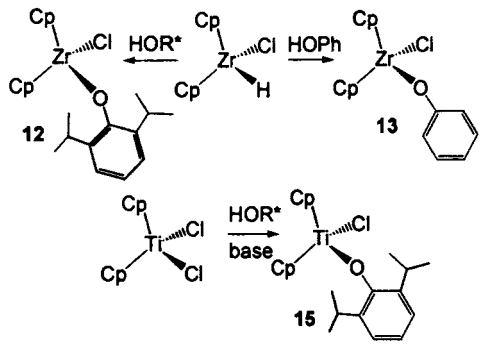


Scheme 4.

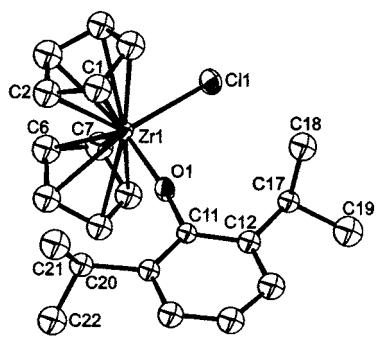


Fig. 6. ORTEP drawing of **12**; 30% thermal ellipsoids are shown and hydrogen atoms are omitted for clarity. Zr(1)–Cl(1) 2.468(4) Å; Zr(1)–O(1) 1.97(1) Å; O(1)–C(11) 1.33(2)°; Cl(1)–Zr(1)–O(1) 99.6(3)°; Zr(1)–O(1)–C(11) 172(1)°.

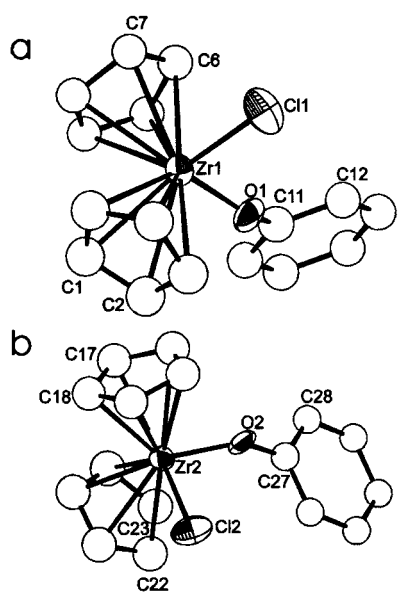


Fig. 7. ORTEP drawing of **13**; 30% thermal ellipsoids are shown and hydrogen atoms are omitted for clarity. Zr(1)–Cl(1) 2.47(1) Å; Zr(1)–O(1) 1.98(3) Å; Zr(2)–Cl(2) 2.45(1) Å; Zr(2)–O(2) 2.01(3) Å; Cl(1)–Zr(1)–O(1) 95.6(9)°; Cl(2)–Zr(2)–O(2) 97.8(8)°; Zr(1)–O(1)–C(11) 149(1)°; Zr(2)–O(2)–C(27) 150(2)°.

While **13** was prepared and characterized, attempts to prepare this compound for catalysis testing were hindered by difficulties in the separation from small amounts of $Cp_2Zr(OC_6H_5)_2$ and $Cp_2ZrCl_2$. In contrast, the species $Cp_2ZrMe(OC_6H_5)$ **14** was readily and cleanly prepared from $Cp_2ZrMeCl$ and LiOPh. In addition, the titanium complex $Cp_2TiCl(OC_6H_3$-*i*-$Pr_2)$ (**15**) was prepared from $Cp_2TiCl_2$ with $HOC_6H_3$-*i*-$Pr_2$ and base (Scheme 4). The $^1$H-NMR spectra of **15** at reduced temperatures show two resonances attributable to the cyclopentadienyl groups as well as two $AX_6$ patterns attributable to the protons of the isopropyl groups. These observations suggest a bent geometry at oxygen and restricted rotation about the Ti–O bond at lower temperatures.

Ethylene polymerizations were performed employing **12**, **14** and **15** with MAO as described above. The results confirm an 11% increase in activity for these aryloxide derivatives compared to the parent metallocenedichlorides. In addition, Repo et al. [25] have recently shown that the activity of $Cp_2ZrCl(OC_6H_3$-*t*-$Bu_2)$ is strongly dependent on the reaction condition. Comparing activities at 30°C and 2 bar ethylene to that at 80°C and 10 bar ethylene, an increase of 30% in activity was observed.

In model reactions of **12** with one equivalent of $AlMe_3$, $^1$H-NMR data confirm that **12** is converted quantitatively to $Cp_2ZrMe(OC_6H_3$-*i*-$Pr_2)$ while addition of a further equivalent of $AlMe_3$ results in the clean conversion to the known complex $Cp_2ZrMe_2$. The aluminum byproduct **9** was also observed by NMR spectroscopy. These model reactions again suggest that alkylation and aryloxide abstraction in the catalytic system generate similar Zr centers.

The increased activity for the aryloxide derivatives suggests that generation of active sites via aryloxide abstraction is more efficient than alkyl abstraction. Alternatively, it may be that transfer of the bulky aryloxide to aluminum enhances charge separation of the active metal-based cationic center from the corresponding counter-anion. It is also interesting to note that while activity is increased, the $M_w$ of the resulting polyethylene is decreased significantly. Although the increased activity may reflect the leaving ability of aryloxide versus halide, the decrease in $M_w$ suggests that aryloxide ligation promotes chain transfer to aluminum and thus premature termination of the polymer.

## 4. Supplementary information

Crystallographic data in CIF format have been deposited with the Cambridge Crystallographic database. (CCDC nos. 121660 to CCDC 121666, inclusive). Copies of this information may be obtained free of charge from: The Director, CCDC, 12 Union Road, Cambridge, CB2 1EZ, UK (Fax: +44-1223-336-033; email: deposit@ccdc.cam.ac.uk or www: http://www.ccdc.cam.ac.uk).

## Acknowledgements

Financial support from the NSERC of Canada is gratefully acknowledged. Bayer Rubber Inc., Sarnia and Nova Chemicals, Calgary are thanked for supplying GPC data.

## References

[1] M. Bochmann, J. Chem. Soc. Dalton Trans. (1996) 255.
[2] Y.-X. Chen, C.L. Stern, T.J. Marks, J. Am. Chem. Soc. 119 (1997) 2582.
[3] P.A. Deck, T.J. Marks, J. Am. Chem. Soc. 117 (1995) 6128.
[4] P.A. Deck, C.L. Beswick, T.J. Marks, J. Am. Chem. Soc. 120 (1998) 1772.
[5] J.P. Mitchell, S. Hajela, S.K. Brookhart, K.I. Hardcastle, L.M. Henling, J.E. Bercaw, J. Am. Chem. Soc. 118 (1996) 1045.
[6] J.H. Gilchrist, J.E. Bercaw, J. Am. Chem. Soc. 118 (1996) 12021.
[7] C. Fritze, M.K. Knickmeier, G. Erker, F. Zaegel, B. Gautheron, P. Meunier, L.A. Paquette, Organometallics 14 (1995) 5446.
[8] M. Knickmeier, G. Erker, T. Fox, J. Am. Chem. Soc. 118 (1996) 40.
[9] M.K. Leclerc, H.H. Brintzinger, J. Am. Chem. Soc. 118 (1996) 9024.
[10] G.C. Bazan, S.J. Donnelly, G. Ridriguez, J. Am. Chem. Soc. 117 (1995) 2671.
[11] G.C. Bazan, G. Ridriguez, J. Am. Chem. Soc. 118 (1996) 2291.
[12] G. Rodriguez, G.C. Bazan, J. Am. Chem. Soc. 119 (1997) 343.
[13] G.C. Bazan, G. Rodriguez, Organometallics 16 (1997) 2492.
[14] T.K. Woo, P.M. Margl, J.C.W. Lohrenz, P.E. Blochl, T. Ziegler, J. Am. Chem. Soc. 118 (1996) 13021.
[15] X.Y. Chen, C.L.Y. Stern, T.J. Marks, J. Am. Chem. Soc. 118 (1996) 12451.
[16] Y. Sun, R.E.V.H. Spence, W.E. Piers, M. Parvez, G.P.A. Yap, J. Am. Chem. Soc. 119 (1997) 5132.
[17] S. Fokken, T.P. Spaniol, H.-C. Kang, W. Massa, J. Okunda, Organometallics 15 (1995) 5069.
[18] D.P. Long, P.A. Bianconi, J. Am.Chem. Soc. 118 (1996) 12453.
[19] T. Tsukahara, D.C. Swenson, R.F. Jordan, Organometallics 16 (1997) 3303.
[20] T.L. Tremblay, S.W. Ewart, M.J. Sarsfield, M.C. Baird, Chem. Commun. (Cambridge) (1997) 831.
[21] A.V. Firth, D.W. Stephan, Organometallics 16 (1997) 2183.
[22] A.V. Firth, D.W. Stephan, Inorg. Chem. 37 (1998) 4726.
[23] A.V. Firth, D.W. Stephan, Inorg. Chem. 37 (1998) 4732.
[24] K. Nomura, N. Naga, M. Miki, K. Yanagi, A. Imai, Organometallics 17 (1998) 2152.
[25] T. Repo, G. Jany, M. Salo, M. Polamo, M. Leskela, J. Organomet. Chem. 541 (1997) 363.
[26] J.R. Strauss, J. Chem. Soc. Chem. Commun. (1965) 567.
[27] G.J. Erskine, G.J.B. Hurst, E.L. Weinberg, B.K. Hunter, J.D. McCowan, J. Organomet. Chem. 267 (1984) 265.
[28] I.M.M. Fussing, D. Pletcher, R. Whitby, J. Organomet. Chem. 470 (1994) 109.
[29] D.M. Healy, J.W. Ziller, A. Barron, J. Am. Chem. Soc. 112 (1990) 2949.
[30] D.T. Cromer, J.B. Mann, Acta Crystallogr. Sect. A Crystallogr. Phys. Theor. Gen. Crystallogr. A 24 (1968) 324.
[31] D.T. Cromer, J.B. Mann, Acta Crystallogr. Sect. A Crystallogr. Phys. Theor. Gen. Crystallogr. A 24 (1968) 390.
[32] B. Cetinkaya, P.B. Hitchcock, H.A. Jasim, M.F. Lappert, H.D. Williams, Polyhedron 9 (1990) 239.